Физика твердого тела, 2016, том 58, вып. 7

16,17

Computational design of multi-states monomolecular device using molecular hydrogen and C_{20} isomers

© *M. Darvish Ganji*

Department of Chemistry, Qaemshahr Branch, Islamic Azad University,
Qaemshahr, Iran

E-mail: ganji_md@yahoo.com

(Received May 20, 2015)

We perform detailed calculations for the interaction of molecular hydrogen with C_{20} isomers in the framework of density functional theory method. The adsorption of H_2 outside the C_{20}-e isomer with parallel orientation with respect to the plane of the hexagon is found to be the most stable adsorption configuration. Thus this might have potential for the hydrogen storing. We have also investigated the number and the position of adsorption sites in the pentagon for the parallel configurations of the H_2/C_{20} systems. We find two stable configurations of the molecule for the C_{20}-bowl isomer that have a small difference in energy. Thus, surprisingly, despite their apparent simplicity these H_2/C_{20}-bowl systems are shown to exhibit the flip-flop motion by a small current pulse. Hence, it might be a candidate for multi-states monomolecular device. Convenient experimental techniques such as field emission microscopy are proposed to test these predictions.

This work was supported by the Azad University of Qaemshahr.

1. Introduction

After the first discovery of C_{60} fullerene [1] in 1985, and carbon nanotube [2] in 1991, various carbon-based nanocage structures, such as fullerene clusters [3–8], single-walled nanotubes [9,10], multi-walled nanotubes [2], nanocapsules [11,12], nanopolyhedra [13], cones [14,15], cubes [16], polyhedra [11] spheres [17], and carbon onions [18], have been studied due to the promising potential for applications in various fields. The characteristic features of their structural formation, physical and chemical properties are of immense interest to the scientific community.

Ever since the discovery of carbon nanotubes (CNTs), vigorous research is going on to explore the tremendous potential of these nanostructures in diverse fields of applications such as flat panel display, microelectronic devices, chemical and electromechanical sensors and fuel cell [19]. One of the recent researches on CNT focuses on its hydrogen storage capacity for several electronic and automotive power sources. These nanomaterials are predicted to be a suitable choice due to its lightweight, high mechanical strength, porous nature and nano size [20]. Between the two possible ways of adsorption like chemisorption and physisorption, latter proves to be a stable and efficient process for hydrogen in carbon nanotubes [21]. Both experimental and theoretical studies exist on the adsorption of molecular and atomic hydrogen in carbon nanotubes [22,23].

The interaction of fullerenes with hydrogen atoms and molecules has also been intensively studied both experimentally [24,25] and theoretically [26–29]. As we know fullerenes, on the other hand, are carbon clusters formed by the closing of a graphitic sheet; the needed curvature is supplied by the insertion, among a given number of graphitic hexagons, of twelve pentagons [30]. Besides its most well-known representative, the nearly spherical C_{60}, a wide variety of fullerenes has been predicted and experimentally observed.

However, as we reduce the number of atoms, these structures become more reactive and unstable: the pentagons present in fullerene-like geometries, although being its major source of interest, are a cause of strain, especially if two of them are neighbors. Small fullerenes, with their high proportion of pentagons, have been actively sought and studied [31]. Recent discoveries include the synthesis and purification of the solid form of C_{36} [3], and the production of the cage and bowl isomers of C_{20} [32]. The vibronic fine structure in photoelectron spectra of the cage has also been recently calculated [33], confirming the previous experimental assignation. These medium-sized carbon clusters are predicted to possess a wide variety of isomers like cages, bowls, planar graphitic structures, rings and linear chains. The theoretical and experimental study of the various isomers is important, because it may help us to better understand the potential capability of these structures for gas storages and molecular electronic devices.

More recently Hata et al. have used field emission microscopy to investigate the behaviour of a single nitrogen molecule on the pentagon at the tip of a carbon nanotube [34]. They observed that the adsorbed nitrogen molecule exhibits a flip-flop motion between two states by a small current pulse, and thus suggested the existence of several adsorption sites originating from the fivefold symmetry in the substrate pentagon. In the line with their study we investigated theoretically, in the previous work [35] the adsorption phenomenon of the nitrogen molecule on pentagon at the tip of a carbon nanotube, looking especially for the number and the positions of adsorption sites in the substrate pentagon.

In this article we investigate theoretically, the adsorption phenomenon of the hydrogen molecule on the C_{20} isomers.

Furthermore, the behaviour of the hydrogen molecule on the pentagon plane of these materials will also be investigated, looking for the number and the positions of adsorption sites in the substrate pentagon that may bring about a novel multi-states monomolecular device.

2. Computational methods

The calculations of the interaction between C_{20} isomers and a hydrogen molecule are carried out using the *ab initio* DFT code SIESTA [36,37]. We use the Perdew–Burke–Ernzerhof (PBE) generalized gradient approximation for the exchange-correlation potential [38]. The core electrons are represented by improved Troullier–Martins pseudopotentials, and a numerical atomic orbitals basis with polarization is used for the valence electrons. Direct diagonalization of Kohn–Sham Hamiltonian is used for the electronic structure calculations. All calculations were done with a double-ξ plus polarization (DZP) basis set.

For simplicity we chose three most stable isomers of the C_{20}: (a) bowl, (b) cage and (c) e-isomers. Geometries of the C_{20} and H_2 are optimized separately prior to the relaxation of the whole system. Structural optimizations are performed until the residual forces become less than $0.01\,\mathrm{eV}\cdot\mathrm{A}^{-1}$.

3. Results and discussion

First we examine the adsorption of a H_2 on the cage isomer. Two possible configurations, named *A* and *B*, were selected for the molecule approaching to the center of a pentagon of carbon atoms: *A* denotes the parallel approach and *B* the perpendicular approach. For the parallel approach *A* the molecule is placed upon the center of a pentagon of carbon atoms with the molecular axis parallel to the surface of the pentagon, while for the perpendicular approach *B* the molecular axis is perpendicular to the pentagon surface. Two configurations are shown in Fig. 1.

The optimized C_{20}-cage structure was used for the molecule adsorption. After full structural optimization of the systems we find that configuration *A* is more stable than the configuration *B*, which corresponds to the parallel approach of the H_2 molecule to the C_{20} on the center of the pentagon of carbon atoms. This is in agreement with the experimental and theoretical results for the similar adsorbed molecule on the pentagon of the similar carbon-based nanostructures [34,35]. It is known that in this configuration the molecule is able to fit optimally into the electron density valley that exists around the pentagon center [39].

The binding energy is calculated from

$$E_b = E_{C_{20}-H_2} - E_{C_{20}} - E_{H_2}, \qquad (1)$$

where $E_{C_{20}-H_2}$ is the total energy of the C_{20} with an adsorbed hydrogen molecule, $E_{C_{20}}$ is the total energy of the pure C_{20} and E_{H_2} is the total energy of the isolated hydrogen molecule.

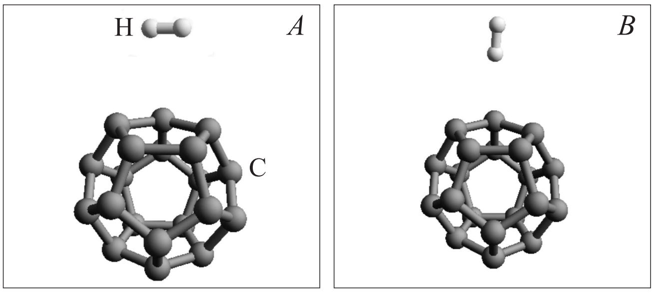

Figure 1. Model for two different adsorption states for a hydrogen molecule on the C_{20}-cage above a pentagon with a molecular axis parallel (*A*) and perpendicular (*B*) to the pentagon surface. White balls: H, gray balls: C.

For the energetically favorable parallel configuration the bond length of H_2 extended to 0.776 Å, which is the basically the same as for an isolated H_2 molecule (0.766 Å). The small extension of the H–H bond is an indication of the weak interaction between the hydrogen molecule and the pentagon of the C_{20}-cage [35]. The calculated binding energy E_b and C–H equilibrium distance are about -0.19 eV (-4.47 kcal/mol) and 2.776 Å, respectively. They are comparable with those of gas adsorption on carbon based nanostructured substrates [40–43] and incorporated molecules into the carbon based nanocapsules [44–48]. The large distance of adsorbed H_2 from the plane and the negative adsorption energy of -0.19 eV indicate weak interaction of H_2 with the pentagon surface of the C_{20}-cage. The calculated binding energy of the perpendicular configuration is about -0.19 eV.

For the bowl isomer we have considered eight configurations: *A*1–*A*8, as depicted in Fig. 2. After full structural optimization of the considered systems we find that configuration *A*5 is the most stable configuration, which corresponds to the parallel approach of the H_2 to the C_{20} on the center of the hexagon of carbon atoms of the concave surface of the bowl isomer. For the *A*5 configuration the bond length of H_2 extended to 0.775 Å, which is similar to the parallel configuration of the cage isomer and is also the same as for an isolated H_2 molecule. The small extension of the H–H bond for this isomer is again an indication of the

Table 1. Calculated binding energies E_b (in eV per adsorbed molecule) for the adsorption of a H_2 molecule on the C_{20}-bowl for the eight configurations of Fig. 2

Configuration	Binding energy, eV
*A*1	−0.09
*A*2	−0.10
*A*3	−0.10
*A*4	−0.12
*A*5	−0.14
*A*6	−0.13
*A*7	−0.13
*A*8	−0.13

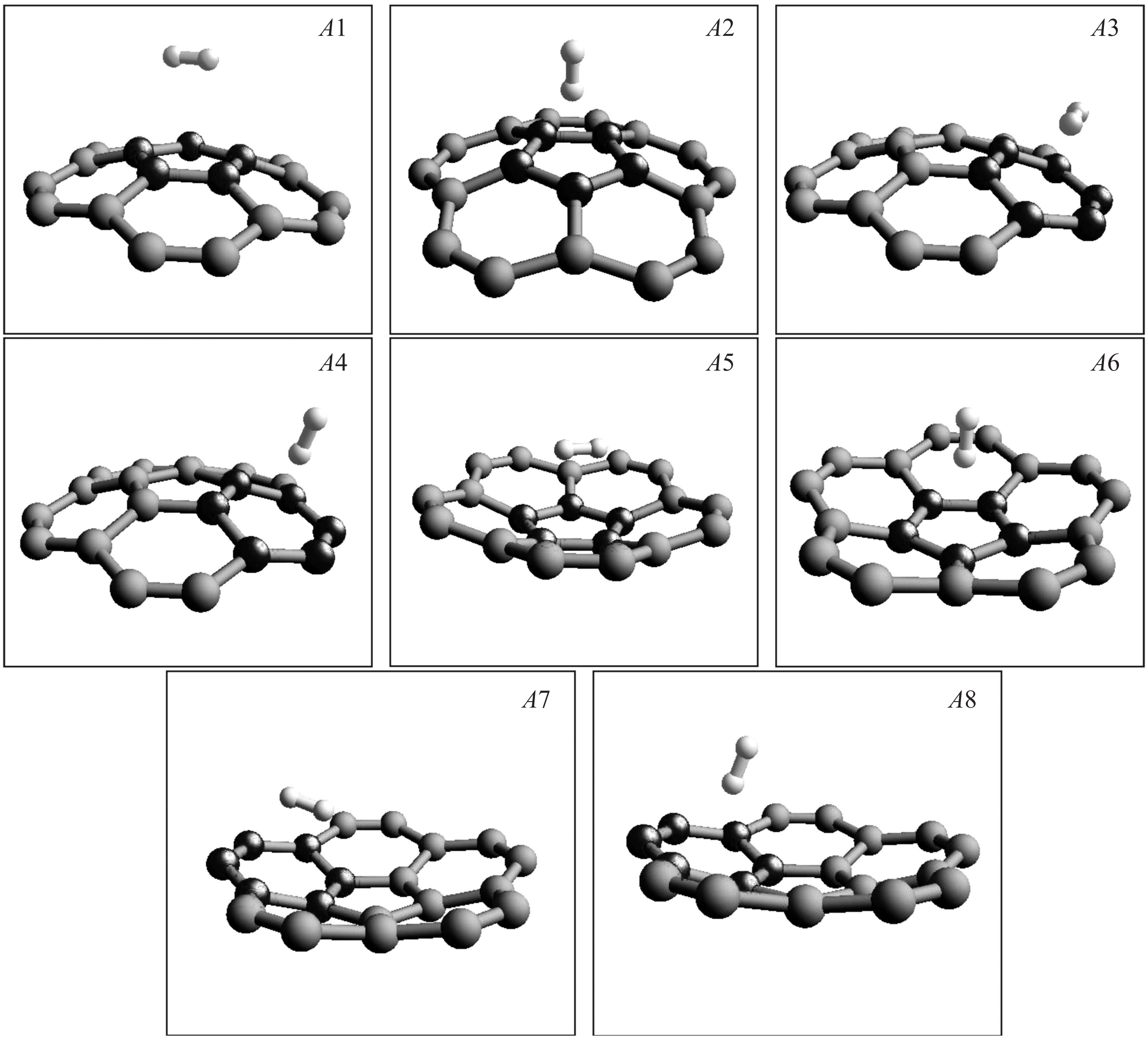

Figure 2. Model for eight different adsorption configurations ($A1$–$A8$) for a hydrogen molecule on the C_{20}-bowl isomer. White balls: H, gray balls: C.

weak interaction between the hydrogen molecule and the pentagon of the C_{20}-bowl. The calculated binding energy E_b and C–H equilibrium distance are about -0.14 eV and 2.710 Å, respectively. The calculated binding energies for all of the considered configurations are summarized in Table 1.

Table 2. Calculated binding energies E_b (in eV per adsorbed molecule) for the adsorption of a H_2 molecule on the C_{20}-e isomer for the six configurations of Fig. 3

Configuration	Binding energy, eV
$B1$	−0.33
$B2$	−0.33
$B3$	−0.30
$B4$	−0.30
$B5$	−0.30
$B6$	−0.30

The third isomer of the C_{20} that has been examined for the adsorption of the H_2 is the C_{20}-e isomer. As it can be seen from the Fig. 3, this isomer has an asymmetric conformation and includes three types of planes: the hexagonal, pentagonal and quadrangular rings. To investigate the adsorption capability of the C_{20}-e isomer, six possible configurations have beon considered. In the first and second configurations the H_2 molecule was placed above the hexagon plane of the C_{20} in the way that the molecular axis was parallel and perpendicular with respect to the ring surface, respectively. For the third–sixth configurations these orientations were considered with respect to the pentagonal and quadrangular rings, respectively, as depicted in Fig. 3.

Similar calculation has been carried out for all of the configurations of Fig. 3. The results show that the parallel orientation of the H_2 with respect to the hexagon plane of the C_{20}-e isomer is the most stable configuration. The calculated binding energy E_b and C–H equilibrium distance are about -0.33 eV and 2.686 Å, respectively. The

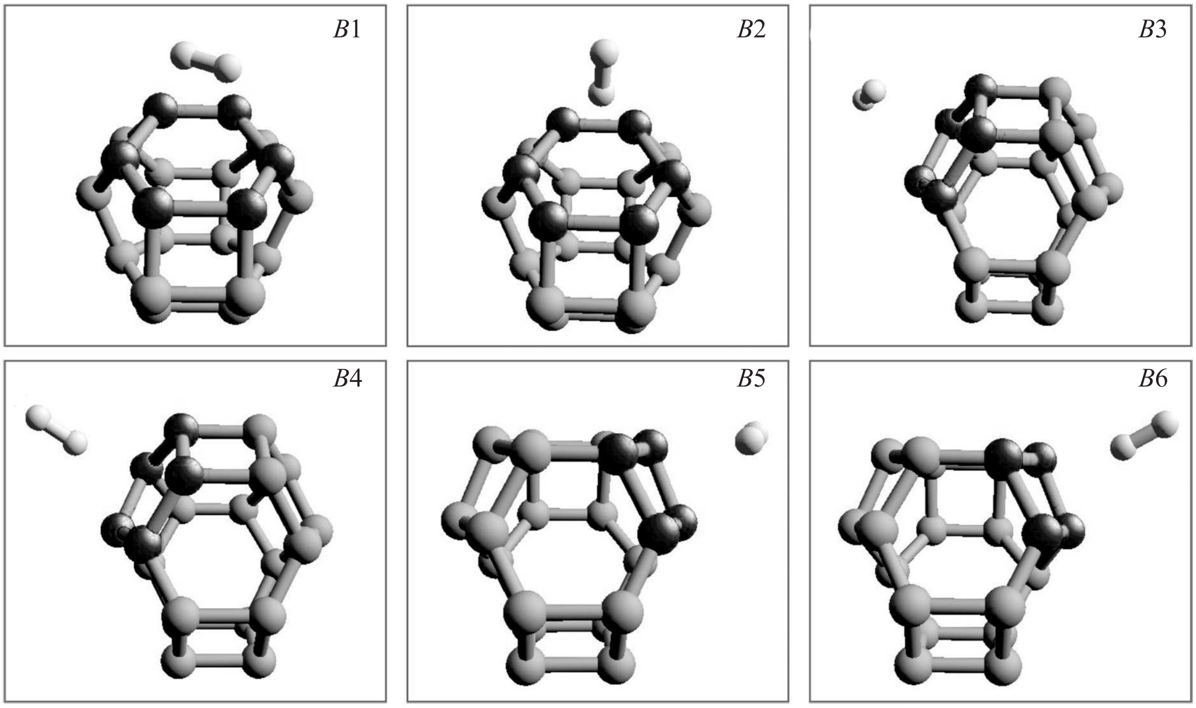

Figure 3. Model for six different adsorption states for a hydrogen molecule on the C_{20}-e isomer above a hexagon, pentagon and quadrangular plane with a molecular axis parallel or perpendicular to the surface ($B1-B6$, respectively). White balls: H, gray balls: C.

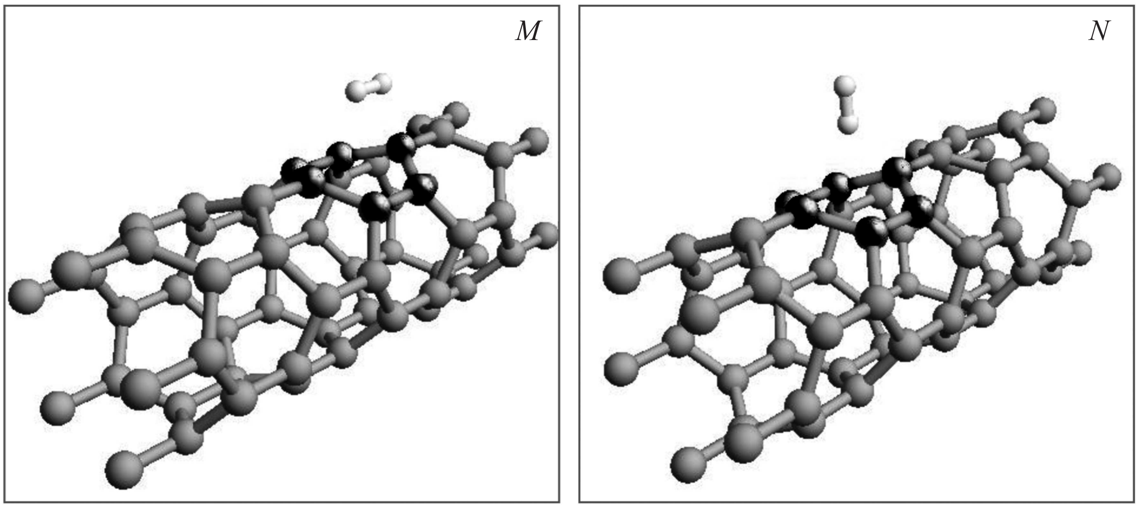

Figure 4. Atomistic configurations of adsorption with the axis of a H_2 molecule parallel (M) and perpendicular (N) to the nanotube axis upon the center of a hexagon of carbon atoms.

calculated binding energy and C−H equilibrium distance of the considered configurations are summarized in Table 2. The binding energy on the hexagon site is considerably higher than that of the adsorption on the pentagon and quadrangle sites. Furthermore, it has also a considerably higher value for E_b in comparison with the other isomers. This indicates that the hexagon plane of the C_{20}-e isomer is the energetically favorable site for H_2 adsorption and hence, the H_2 adsorption capability of C_{20}-e isomer is better than that of other isomers.

In order to compare the capability of the C_{20} isomers for hydrogen adsorption with the carbon nanotubes we also investigate the adsorption of H_2 on a $(5,0)$ zigzag CNT of very high curvature. Two possible configurations, named M and N, were selected for the molecule approaching to the center of a hexagon of carbon atoms: M denotes the parallel approach and N the perpendicular approach. For the parallel approach M the molecule is placed upon the center of a hexagon of carbon atoms with the molecular axis parallel to the surface of the hexagon, while for the perpendicular

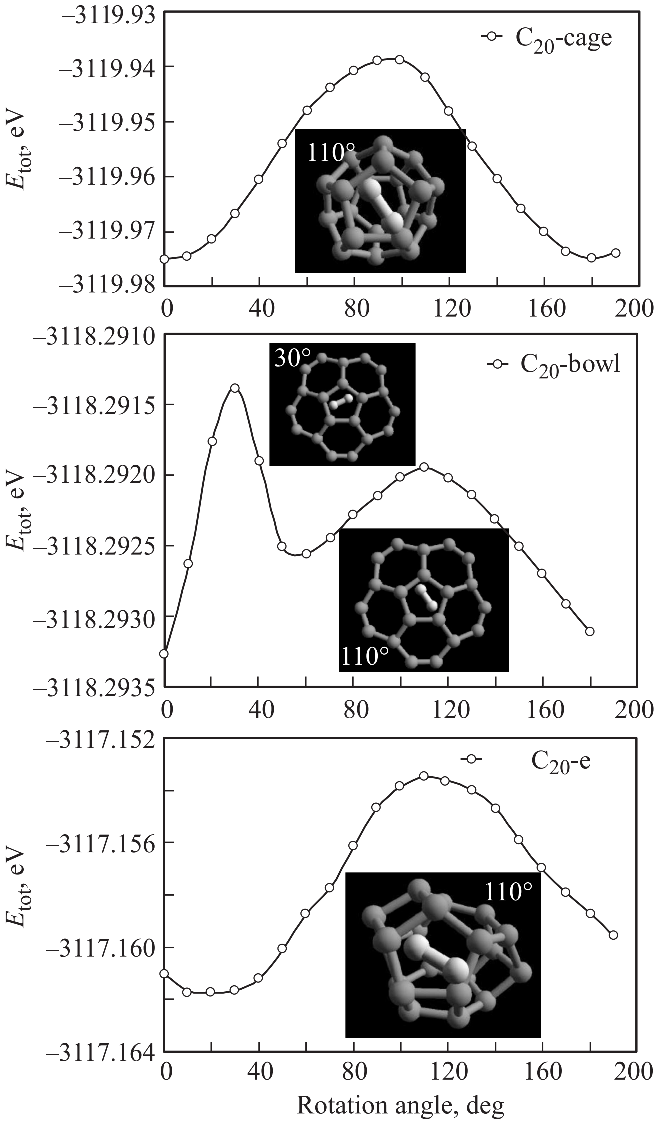

Figure 5. Calculated barrier energy curve for the transition between the lowest energy and the metastable states for the H_2/C_{20} systems. The clock-wise rotation of the H_2 molecule along the pentagon center by 10° was implemented in each scan process.

approach N the molecular axis is perpendicular to the hexagon surface. Two configurations are shown in Fig. 4.

The results show that the parallel ($E_b = -0.24\,\text{eV}$) configuration of the H_2 with respect to the hexagon plane of the CNT is the more stable than the perpendicular one ($E_b = -0.23\,\text{eV}$). As we can see, on the other hand, the binding energy of the C_{20}-e isomer is considerably higher than that of the adsorption on the other C_{20} isomers and also on the carbon nanotube. This indicates that the C_{20}-e isomer has the energetically favorable site for H_2 adsorption. Hence, the H_2 adsorption capability of C_{20}-e isomer is better than that of other isomers and carbon nanotubes.

In the remaining part of this article we focus on the behaviour of adsorbed H_2 on the pentagon of the C_{20} isomers looking for the flip-flop motion that may bring about a novel multi-states monomolecular device. In order to investigate the flip-flop motion of the adsorbed H_2 molecule on the pentagon plane we rotate the H_2 molecule from its most stable state for all of the parallel configurations, following Refs [34] and [35]. The pentagon plane axis corresponds to the rotation axis, and we rotated the molecule in discrete steps of 10° together with a rotation angle range from 0 to 180°. At each rotation step we have calculated the total energy of the whole system.

Fig. 5, $a-c$ show the scanned potential curve of the C_{20}-cage, C_{20}-bowl and C_{20}-e systems, respectively. We find one lowest energy configuration for C_{20}-bowl isomer only, at 0 and a metastable configuration at 60° that display a similar behaviour in comparison with the adsorbed N_2 on the pentagon of the capped CNT [34,35]. This might have potential for multi-states monomolecular device. The corresponding ball-and-stick models of these configurations are also represented in the figure.

The results also show that the two-atomic molecules such as H_2 (and N_2 [34,35]) can exhibit a flip-flop motion when they were adsorbed on the pentagon ring which was surrounded by the hexagon rings as seen for the bowl isomer of the C_{20} but not for the cage and e isomers. Hence we expect a similar behaviour for the adsorbed H_2 or N_2 molecule on the C_{60} fullerene that includes pentagonal planes surrounded by the hexagonal rings. Convenient experimental techniques such as field emission microscopy are proposed to test these predictions.

4. Conclusions

We have theoretically studied the adsorption of a single hydrogen molecule on the C_{20} isomers using DFT calculations. We have investigated three isomers of the C_{20}: the cage, bowl and e isomers. The results showed that the H_2 molecule preferred to be adsorbed on the hexagon of the C_{20}-e isomer in the parallel orientation. The H_2 adsorption capability of C_{20} isomers has also been compared with the carbon nanotubes. Our first principles calculations predicted that the H_2 adsorptive capability of C_{20}-e isomer is higher than that of other C_{20} isomers and carbon nanotubes.

Furthermore, the number and the position of adsorption sites in the pentagon plane of the C_{20} isomers, which leads to the precise control of adsorption states, have also been studied for the parallel orientations. We have rotated the H_2 molecule from its most stable state for all of the parallel configurations of H_2/C_{20} systems. The calculations showed that two metastable states are more stable than the others for the C_{20}-bowl isomer only, thus these might be the preferred adsorption sites. The barrier energy between these configurations indicated that a very small energy is needed for the transition between the two most stable states. This confirms the experimental results of Hata et al. for the N_2 adsorbed on the pentagon of the capped CNT in reference [34], where they found that a small current pulse caused the transition between two states. Thus we predicted the possible switching states for the H_2 adsorbed on the pentagon of the C_{20}-bowl isomer. This can lead to the precise control of adsorption states, and consequently may bring about a novel multi-states monomolecular device. We hope that the ideas put forward here will facilitate bridging the gap between theory and molecular electronics experiments.

We thank Prof. S. Sanvito and I. Rungger for many fruitful discussions.

References

[1] H.W. Kroto, J.R. Heath, S.C. O'Brien, R.F. Curl, R.E. Smalley. Nature **318**, 162 (1985).
[2] S. Iijima. Nature **354**, 56 (1991).
[3] C. Piskoti, J. Yarger, A. Zettl. Nature **393**, 771 (1998).
[4] R.E. Smalley. Acc. Chem. Res. **25**, 98 (1992).
[5] J. Hunter, J. Fye, M.F. Jarrold. J. Phys. Chem. **97**, 3460 (1993).
[6] C. Rohlfing, J. Kaldor. Chem. Phys. Lett. **81**, 3322 (1984).
[7] W. Krätschmer, L.D. Lamb, K. Fostiropoulos, D.R. Huffman. Nature **347**, 354 (1990).
[8] F. Diederich, R.L. Whetten. Acc. Chem. Res. **25**, 119 (1992).
[9] S. Iijima, T. Ichihashi. Nature **363**, 603 (1993).
[10] D.S. Bethune, C.H. Kiang, M.S. de Vries, G. Gorman, R. Savoy, J. Vazquez, R. Beyers. Nature **363**, 605 (1993).
[11] R.S. Ruoff, D.C. Lorents, B. Chan, R. Malhotra, S. Subramoney. Science **259**, 346 (1993).
[12] Y. Saito, T. Yoshikawa, M. Inagaki, M. Tomita, T. Hayashi. Chem. Phys. Lett. **204**, 277 (1993).
[13] T. Oku, T. Hirano, M. Kuno, T. Kusunose, K. Niihara, K. Suganuma. Mater. Sci. Eng. B **74**, 206 (2000).
[14] A. Krishnan, E. Dujardin, M.M.J. Treacy, J. Hugdahl, S. Lynum, T.W. Ebbesen. Nature **388**, 451 (1997).
[15] K. Sattler. Carbon **33**, 915 (1995).
[16] Y. Saito, T. Matsumoto. Nature **392**, 237 (1998).
[17] Y. Saito, T. Yoshikawa, M. Okuda, N. Fujimoto, K. Sumiyama, K. Suzuki, A. Kasuya, Y. Nishina. J. Phys. Chem. Solids **54**, 1849 (1993).
[18] D. Ugarte. Nature **359**, 707 (1992).
[19] M.S. Dresselhause, G. Dresselhaus, P.C. Eklund. Science of fullerenes and carbon nanotubes. Academic Press, N.Y. (1996).
[20] O. Gülseren, T. Yildirim, S. Ciraci. Phys. Rev. Lett. **87**, 116 802 (2001).
[21] J.A. Alonso, J.S. Arellano, L.M. Molina, A. Rubio, M.J. Lopez. IEEE Trans Nanotechnol. **3**, 304 (2004).
[22] A.C. Dillon, K.M. Jones, T.A. Bekkeduhl, C.H. Kiang, D.S. Bethune, M.J. Heben. Nature **386**, 377 (1997).
[23] J.S. Arellano, L.M. Molina, A. Rubio, M.J. Lopez, J.A. Alonso. J. Chem. Phys. **117**, 2281 (2002).
[24] T. Takenobu, M. Shiraishi, A. Yamada, M. Ata, H. Kataura, Y. Iwasa. Synth. Met. **135**, 787 (2003).
[25] R.E. Haufler, J. Conceicao, L.P.F. Chibante, Y. Chai, N.E. Byrne, S. Flanagan, M.M. Haley, S.C. O'Brien, C. Pan, Z. Xiao, W.E. Billups, M.A. Ciufolini, R.H. Hauge, J.L. Margrave, L.J. Wilson, R.F. Curl, R.E. Smalley. J. Phys. Chem. **94**, 8634 (1990).
[26] G. Seifert. Solid State Ionics **168**, 265 (2004).
[27] L. Türker, S. Erko¸ J. Mol. Struct.: Theochem **638**, 37 (2003).
[28] B.I. Dunlap, D.W. Brenner, J.W. Mintmire, R.C. Mowrey, C.M.T. White. J. Phys. Chem. **95**, 5763 (1991).
[29] G.E. Scuseria. Chem. Phys. Lett. **176**, 423 (1991).
[30] H.W. Kroto. Int. J. Mass Spectrom. Ion Process **138**, 1 (1994).
[31] A. van Orden, R.J. Saykally. Chem. Rev. **98**, 2313 (1998).
[32] H. Prinzbach, A. Weiler, P. Landenberger, F. Wahl, J. Wőrth, L.T. Scott, M. Gelmont, D. Olevano, B. Issendorff. Nature **407**, 60 (2000).
[33] M. Saito, Y. Miyamoto. Phys. Rev. Lett. **87**, 035 503 (2000).
[34] S. Waki, K. Hata, H. Sato, Y. Saito. J. Vac. Sci. Technol. B **25**, 517 (2007).
[35] M.D. Ganji. Nanotechnology **19**, 025 709 (2008).
[36] J.P. Perdew, K. Burke, M. Ernzerhof. Phys. Rev. Lett. **77**, 3865 (1996).
[37] P. Ordejon, E. Artacho, J.M. Soler. Phys. Rev. B **53**, 10 441 (1996).
[38] J.M. Soler, E. Artacho, J.D. Gale, A. Garcýa, J. Junquera, P. Ordejon, D. Sánchez-Portal. J. Phys.: Condens Matter **14**, 2745 (2002).
[39] J.S. Arellano, L.M. Molina, A. Rubio, J.A. Alonso. J. Chem. Phys. 112, 8114 (2000).
[40] I. Cabria, M.J. Lopez, J.A. Alonso. Eur. Phys. J. D **34**, 279 (2005).
[41] M.D. Ganji. Phys. Lett. A **372**, 3277 (2008).
[42] M.D. Ganji, A. Mirnejad, A. Najafi. Sci. Technol. Adv. Mater. **11**, 045 001 (2010).
[43] M. Darvish Ganji, M. Mohseni, A. Bakhshandeh. J. Mol. Model **19**, 1059 (2013).
[44] M. Darvish Ganji, S.M. Hosseini-khah, Z. Amini-tabar. Phys. Chem. Chem. Phys. **17**, 2504 (2015).
[45] M.D. Ganji. Physica E **41**, 1433 (2009).
[46] M.D. Ganji, M. Mohseni, O. Goli. J. Mol. Struct.: Theochem **913**, 54 (2009).
[47] M.D. Ganji. Fulleren. Nanotubes Carbon Nanostruct. **18**, 24 (2010).
[48] M.D. Ganji, M. Rezvani, M. Shokry, A. Mirnejad. Fulleren. Nanotubes, Carbon Nanostruct. **19**, 421 (2011).